

# S.U.R.E: Soft Upper-Limb Rehabilitation Exoskeleton

Samar Bahrami

*Mechanical and Aerospace Engineering*  
University of Virginia  
Charlottesville, VA  
ssb7xqj@virginia.edu

Alison Butcher

*Mechanical and Aerospace Engineering*  
University of Virginia  
Charlottesville, VA  
apb3gt@virginia.edu

Caroline Flanagan

*Mechanical and Aerospace Engineering*  
University of Virginia  
Charlottesville, VA  
ccf3sb@virginia.edu

Caroline Nealon

*Mechanical and Aerospace Engineering*  
University of Virginia  
Charlottesville, VA  
cen6ghx@virginia.edu

Kathryn Zimmnick

*Mechanical and Aerospace Engineering*  
University of Virginia  
Charlottesville, VA  
kmz8a@virginia.edu

**Abstract**— S.U.R.E, an acronym for soft upper-limb rehabilitation exoskeleton, is designed for patients who have lost mobility in their upper-limb in an effort to improve and restore their mobility. The current design was inspired by current products and techniques in clinical practice, and improved upon in hopes of resolving the shortcomings that have not been accounted for previously. The main goal this design sought to accomplish is to make robotic rehabilitation therapy usable at-home, and without the help of a healthcare worker or engineer. Prioritizing at-home use means that accessibility features must be incorporated, including a lightweight design, low cost, portability, and ease of operation.

The exoskeleton alternates between two motions: flexion of the elbow while the hand clamps into a fist, and extension of the elbow as the hand stretches back out. This combination of fine and large motor skills is an important component of the at-home rehabilitation exo that is missing in current practice. Combining these two motions saves time and expands the applications of the machine itself. Only four components will come into contact with the wearer: a small runner's backpack, a wrist cuff, a compression glove, and a small push button. By using textiles, traditional use of hard plastics and metals to provide structural support is not necessary; instead, Bowden cables controlled by small motors in the backpack and glove will direct the movements. User-set maximum and minimum elbow angles help ensure that the biomechanics of the design are safe and usable for a wide range of populations. The elbow and hand motors are controlled by a microcontroller in the backpack which utilizes PID motor control. Using small DC motors and microcontrollers allows the design to run independently of any computer and light enough to carry in a backpack, making it fully portable.

The user progresses through the physical therapy session by pressing a small push button that is accessible when wearing the backpack. The design's adaptability to patient circumstances counteracts the main issues facing the standard robotics used for rehabilitation. By eliminating the need for outpatient visits, the cost of rehabilitation and the physical barrier to accessing therapy is reduced. The current design was inspired by previous designs in contemporary biomechanical engineering research and improved upon in hopes of resolving the shortcomings that had not been accounted for previously. Additionally, S.U.R.E. is designed as an affordable alternative to traditional outpatient and inpatient rehabilitation.

**Keywords**—stroke, exoskeleton, rehabilitation, robot, Arduino

## I. INTRODUCTION

Stroke is a leading cause of disability in the worldwide adult population and, according to the American Heart Association [13], approximately 3.83 million Americans are estimated to be living with a stroke related disability. Although full recovery is unlikely for stroke survivors, full or even partial rehabilitation can be achieved. A high percentage of patients recovering from stroke have upper-limb disability, including fine motor movements in the hand, like grasping, and larger functions like flexion and extension of the elbow. Fortunately, these impairments can be significantly reduced or even negated with repetitive task training in which the patient undergoes the same simple motion continuously as a means of relearning the motion, gaining muscle, and most importantly reestablishing the mind-muscle connection. High doses of this repetitive training have been demonstrated as a key factor in recovering and maintaining mobility. Due to the repetitive nature, robotics and technological approaches to rehabilitation mechanisms are a promising alternative to traditional physical therapy, and may even reduce impairment to a greater degree [14].

### A. Timeline

The beginning of this process in September entailed completing a literature review of similar research. Several academic journal articles about robotic assistive exoskeletons were read to try and ascertain what research had already been completed, what these groups had learned, and what gaps in this field still need to be addressed. This was followed by an analysis of the gaps in research and brainstorming about possible projects. In October, the conceptual design was finalized and the first materials needed to construct the prototype were ordered. The code was written, the Arduino board was designed, materials were sewn together, design of the motor mounts and Arduino board mounts on CAD software commenced in November.

Ordering materials and troubleshooting code and Arduino board assembly continued into February and March. Testing the motor control, ergonomics, and safety of the device occurred in April. During May, bug fixes and alterations to the textiles were conducted. The final design was completed the first week of May.

## SEMG-Driven Soft ExoSuit

### B. Literature review

This research project investigates the gaps in current robotic stroke rehabilitation technologies, mainly within the realm of stroke rehabilitation access. In an attempt to develop a robotic exoskeleton to mitigate these shortcomings, literature on the topic of hand and arm assistive-robotic devices has been researched. The need for affordable stroke rehabilitation technology that is comfortable and accessible at-home has been recognized. Currently, there is a lack of soft robotic exoskeleton designs, especially fine motor rehabilitation designs. Typical designs are incredibly expensive, hard robots, which are only available to patients at hospitals and physical therapy offices. The current standards of rehabilitation robots lack key aspects that increase the accessibility of rehabilitation: portability, cost, ease of use, adjustability, comfort, and broadness of treatment.

### Hybrid Soft-Rigid Hand Exoskeleton

Researchers at the Harbin Institute of Technology developed a soft-rigid hand exoskeleton for fine motor stroke rehabilitation. This device allows for more precise mathematical modeling than a soft design due to its hybrid nature, while still maintaining more comfort than hard exoskeletons.

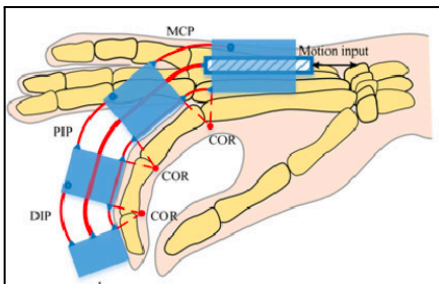


Fig. 1 Harbin Institute of Technology, Hybrid Soft-Rigid Hand Exoskeleton

This design supports fine motor rehabilitation, a feature S.U.R.E. could benefit from; however it is not as ergonomic as it could be because of the rigid components [6].

### RUPERT: Robotic Upper-Extremity Repetitive Therapy

Another proposed design for upper-limb rehabilitation exoskeleton is RUPERT: Robotic Upper-Extremity Repetitive Therapy by Sugar et. al [11]. This exoskeleton allows for multiple degrees of motion.

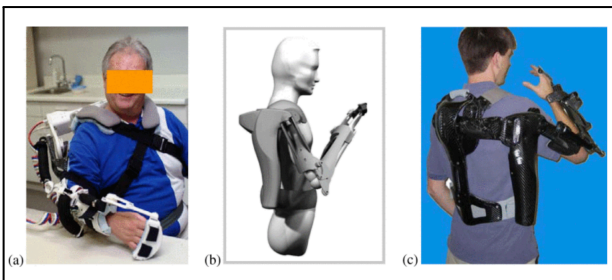


Fig. 2 Sugar et al., RUPERT

Although effective for stroke rehabilitation, this design is expensive and impractical for long periods of use (Sugar et.al).

The ExoSuit proposed by Hosseini et al. [5]. focuses on a soft, lightweight design that compensates for the effort expended by the wearer's upper body, allowing them to carry more weight for a longer period of time.

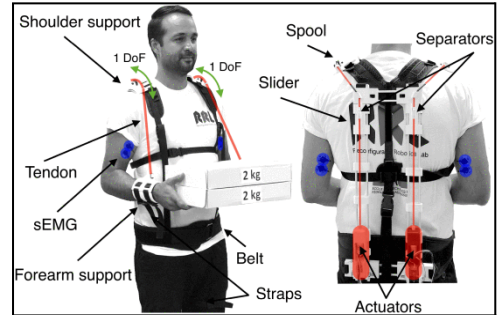


Fig. 3 Reconfigurable Robotics Lab, SEMG-Driven Soft ExoSuit

While it is under four pounds, it is not compact, which restricts the ability to work while wearing it. There is also only one degree of freedom, so only one motion, flexion and extension of the elbow, is supported.

### Practical Exosuit Design for Patients with Amyotrophic Lateral Sclerosis

This is a soft exoskeleton design developed through previous research at the University of Virginia [9]. This design is comfortable and lightweight, as well as affordable, achieving key design considerations; however, the device is limited to only one degree of freedom. It allows only elbow flexion and extension, and does not include support for fine motor rehabilitation, a potential concern for patients in stroke rehabilitation. Additionally, the inclusion of EMG sensors makes this design difficult to use for people who do not have a background in using these devices and analyzing their signals.

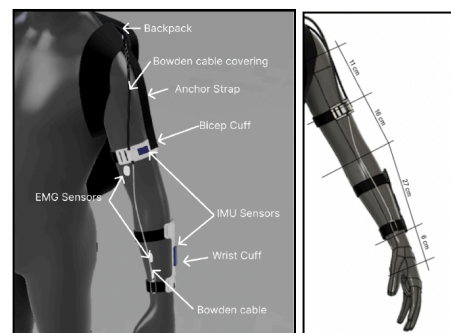


Fig. 4 UVA Mechanical and Aerospace Engineering Department, Upper Limb Soft Exoskeleton Design

### C. Background

Stroke victims often exhibit paresis of the upper limb on either side of the body. A common rehabilitation method is constraint-induced movement therapy, abbreviated as CIMT, where the paretic arm performs repetitive functional activities whilst the unimpaired arm is physically restrained [6]. For the upper extremity, this consists of flexion and extension of the arm and fine motor movement of the hands and fingers. In a study performed to determine the effectiveness of CIMT, it was found that after one year the participants performed better

on a series of timed, semi-functional tasks and on overall hand function. Additionally, after two years the participants did not exhibit any signs of decline, rather trending towards continued improvement [7]. However, the benefits of CIMT come at a cost to both the patient and the personnel providing the rehabilitation. In the study conducted above, the physical therapists provided six hours of rehabilitation every day for five days a week, putting an immense amount of fatigue on the therapists. In regards to the patient, the financial burden of stroke rehabilitation cannot be afforded by the majority of stroke victims. A research paper published in the Journal of Rehabilitation Medicine estimated that the average cost for inpatient and outpatient stroke rehabilitation was \$70,601 and \$27,473, respectively [12]. The disadvantages of stroke rehabilitation are often neglected in the grand scheme of restoring mobility to stroke victims, however providing solutions to these problems allows a wider range of accessibility to rehabilitation and less of a burden to both parties.

#### D. Goal

S.U.R.E: Soft Upper-limb Rehabilitation Exoskeleton has been developed to address the gaps listed above. The objective was to design a rehabilitation mechanism for upper-limb stroke disability that addresses problems relating to stroke care access. Specifically, the design will be made from affordable materials costing no more than \$300, and weighing less than 5 lbs. The design will be easily operable by the wearer, so that it can be used at-home and reduce the need for in-patient and out-patient rehabilitation care.

To expand the reach and scope of the exoskeleton, it will cover two motions important to rehabilitation, and be applicable to a range of body types. Flexion and extension of the elbow and grasp and extension of the hand are two motions important to upper-limb rehabilitation physical therapy. S.U.R.E. will be more ergonomic and wearable compared to its hard counterparts by using flexible and soft materials while minimizing the use of hard metals and plastics. As a result of these factors, accessibility as well as the frequency and duration of care can be increased as opposed to typical physical therapy, and consequently make strides towards increasing rates of stroke rehabilitation.

## II. METHODS AND MATERIALS

### A. Design

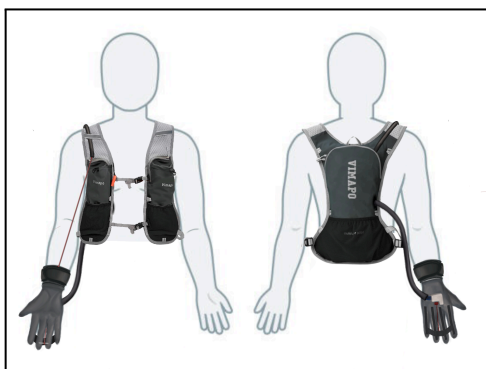


Fig. 5 A digital mock up of the completed design as viewed from the front and back

The exoskeleton features a soft, ergonomic design which is suitable for individual, at-home use. This design is

composed of a 1.5 liter backpack and a glove with an attached wrist cuff. The use of a Bowden cable, motor, and Arduino are inspired by the 2022 design team [9]. Access to this research paper and Arduino code provides a reference to check torque calculations and required coding components. The backpack houses a circuit board and a motor mounted on a 3D printed backpack insert.

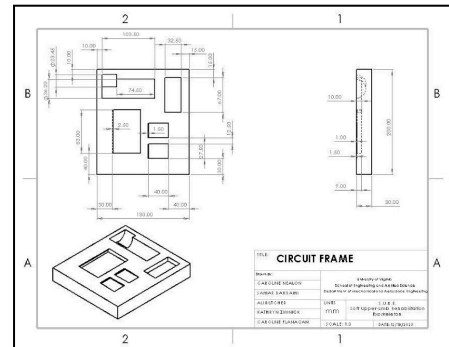


Fig. 6 Drawing of Backpack Insert

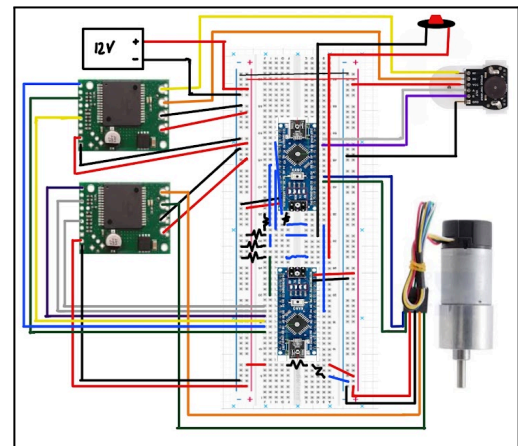


Fig. 7 Circuit Diagram

The backpack insert depicted in Figure 7 includes compartments for the breadboard, two motor controllers, and the elbow motor. It also has space for a 3D printed reel attachment for the motors depicted in Figure 8 and 9. The smaller motor will be fixed to the back of the glove above the knuckles of the fourth and fifth fingers and will have a similar reel. The breadboard is used to connect the electronic design components to two Arduino Nanos, which are programmed to control the entire system. Power is given to the system via a battery pack located outside of the backpack that contains a switch. Since this is the only source of power given to the device, the switch can also act as an emergency stop if needed.

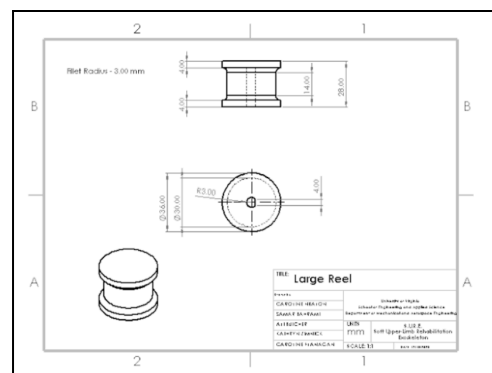


Fig. 8 Drawing of the reels for the large motor

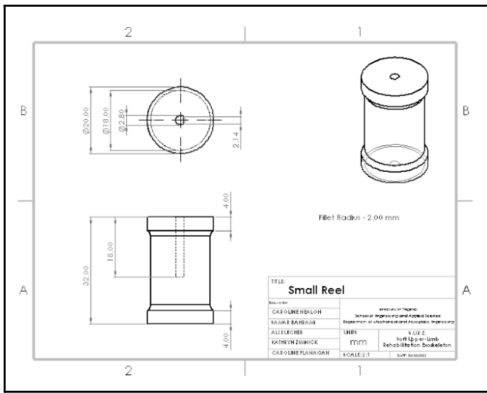


Fig. 9 Drawing of the reels for the small motor

The wires for the push button, battery pack, and small motor extend from the backpack, with the hand motor wires coming from the bottom right corner as seen in Fig. 5. Wire conduits were used to keep these wires organized and protected as the user interacts with them and motion is performed. The push button's wires come over the left shoulder and through tabs along the backpack's strap, so that it is easily accessible on the side not performing rehabilitation. The button is used to start and calibrate the design. The battery pack's wiring also goes through the tabs in the left backpack sleeve, so that the battery pack can sit in a pocket on the left sleeve and be easily accessed in case an emergency stop is needed. A full assembly of the circuit board and backpack insert is depicted in Figure 10.

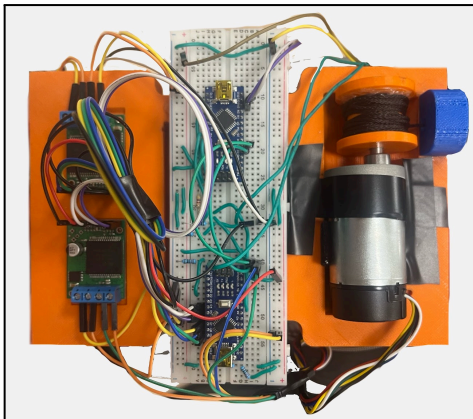


Fig. 10 Assembled backpack insert and circuit board

The reels on the hand motor and elbow motor will allow for the smooth retraction of paracord cables guided by bicycle brake line tubing. These cables serve to translate the rotation of the motors into the movement of the forearm and fingers. The cable responsible for elbow movement is attached at the wrist. A fabric loop used in conjunction with a cord lock allows the cable length to be adjusted for users with a variety of arm lengths and secures the cable without causing uncomfortable rubbing. The cable responsible for finger movement is attached to a fabric strip at the fingertips.

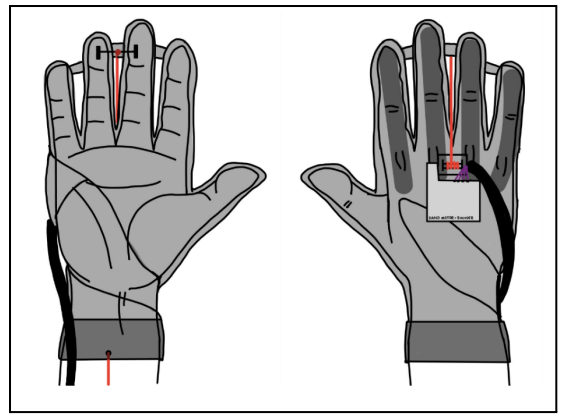


Fig. 11 A digital mock up of the completed design viewed from the front and back of the hand



Fig. 12 Glove and wrist cuff viewed from the front and back of the hand

To fabricate the glove designed in Figure 11, a compression glove was sewn onto a neoprene armband. Elastic was sewn onto the fingers of the compression glove, to facilitate the return of the fingers into their resting position. The fabricated gloves are depicted in Figure 12.

### B. Torque Calculations

Torque calculations were completed to ensure that the motors have enough torque to achieve elbow flexion and extension and fine motor movement of the hand. In order to determine the torque required for elbow flexion and extension, the rotation of the lower arm about the elbow was modeled as a third-class lever. A third-class lever is a lever where the fulcrum is at one end, a weight is on the opposite end, and forces are applied between the fulcrum and weight. The elbow joint is the fulcrum and the weight that it needs to overcome in order to rotate are the weights of the forearm and the hand.

There are three muscles that are involved in overcoming the resistance of the forearm and hand: biceps brachii, brachialis, and the brachioradialis.

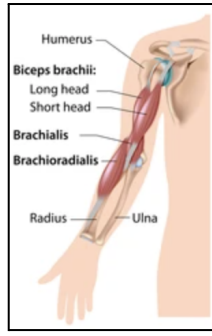


Fig. 13 Diagram depicting insertions of biceps brachii, brachialis, and brachioradialis on the lower arm.

With the forces acting on the lower arm established, the free-body diagram can be depicted as follows:

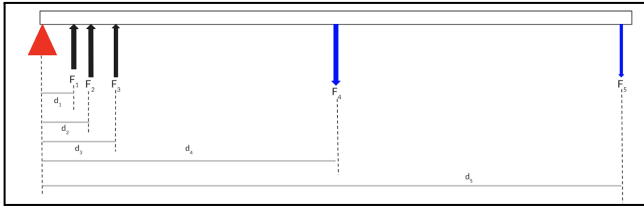


Fig. 14 Free-body diagram of lower arm

The corresponding muscles for each subscript have been tabulated below:

TABLE I

SUBSCRIPT AND CORRESPONDING MUSCLE AND MOMENT ARM

Subscript	Corresponding Muscle	Moment Arm
1	Biceps Brachii	$d_1$
2	Brachialis	$d_2$
3	Brachioradialis	$d_3$
4	Forearm	$d_4$
5	Hand	$d_5$

Taking counterclockwise rotation to be positive, the torque about the elbow can be calculated yielding the following equation:

$$\sum T = F_1 d_1 + F_2 d_2 + F_3 d_3 - F_4 d_4 - F_5 d_5 = 0 \quad (1)$$

Since  $F_4$  and  $F_5$  are essentially the weights of the forearm and hand, respectively, these values can be quantified from prior research on the human body. However for  $F_1$ ,  $F_2$ , and  $F_3$  there is no single value that can be used as the force exerted by each muscle can take on a range of values. Thus, a valid assumption would be to determine the maximum force that can be produced by each muscle. With this assumption, the output forces can be related to each muscle's physiological cross-sectional area (PCA). The PCA is defined to be the volume of the muscle divided by its fiber length, and conveniently is proportional to the maximum output force of

the muscle, i.e.  $F_{\max} \propto PCA$  [1]. Therefore,  $F_1$ ,  $F_2$ , and  $F_3$  can be rewritten as some proportionality constant  $k_i$  multiplied by the PCA of each muscle,  $A_i$ . Eq. 1 can now be modified to:

$$k_1 A_1 d_1 + k_2 A_2 d_2 + k_3 A_3 d_3 = W_4 d_4 + W_5 d_5 \quad (2)$$

Take note that  $F_4$  and  $F_5$  were replaced with their respective weights, as justified previously. Although the muscle forces were able to be related to one of their intrinsic properties, Eq. 2 is not solvable for a given variable because there are three separate  $k$  values. However, the quantities of interest are the output forces produced by the muscles and the resistances of the forearms and hands. These can be solved by assuming that the  $k$ 's are all equal to one another. Thus, Eq. 2 can be rearranged to solve for  $k$  in terms of known values.

$$k = \frac{W_4 d_4 + W_5 d_5}{A_1 d_1 + A_2 d_2 + A_3 d_3} \quad (3)$$

The output forces can now be solved by multiplying the PCA of each muscle by the  $k$  factor from Eq. 3.

$$F_1 = k A_1 = \left( \frac{W_4 d_4 + W_5 d_5}{A_1 d_1 + A_2 d_2 + A_3 d_3} \right) A_1 \quad (4)$$

$$F_2 = k A_2 = \left( \frac{W_4 d_4 + W_5 d_5}{A_1 d_1 + A_2 d_2 + A_3 d_3} \right) A_2 \quad (5)$$

$$F_3 = k A_3 = \left( \frac{W_4 d_4 + W_5 d_5}{A_1 d_1 + A_2 d_2 + A_3 d_3} \right) A_3 \quad (6)$$

The weights of the forearm and hand were determined from empirical research. Values for each variable can be found in Table II and Table III. An important clarification for Table III is that the weights of the forearm and hand were found as a percentage of the average body weight of the American male and female. As a precaution against underdesigning, the weights of the forearm and hand were taken to be the values calculated from using the average body weight of the American male since these values are both greater than that of the females. These values were taken from Plagenhoef et.al [10] and the weight values used are designated in bold in Table III. The values in Table II are referenced from Herman [4].

TABLE II

VALUES FOR MOMENT ARMS AND PHYSIOLOGICAL CROSS-SECTIONAL AREAS

Muscle	Moment Arm (cm)	PCA (cm <sup>2</sup> )
Biceps Brachii	4.6	4.6
Brachialis	3.4	7.0
Brachioradialis	7.5	1.5
Forearm	14.15	N/A
Hand	33.5	N/A

TABLE III  
WEIGHTS OF FOREARM AND HAND

		Male	Female
<b>Average Body Weight (lbs)</b>		199.8	170.8
<b>Forearm</b>	Percentage of Total Body Weight (%)	1.62	1.38
	Weight (lbs)	<b>3.24</b>	2.36
<b>Hand</b>	Percentage of Total Body Weight (%)	.61	.56
	Weight (lbs)	<b>1.22</b>	.96

The output force from the muscles were calculated by plugging in the values from Tables II & III into Eqs. 4,5, and 6. The results are found in Table IV.

TABLE IV  
RESULTS FOR MAXIMUM OUTPUT FORCES

Muscle	Force (lbf)
Biceps Brachii	7.08
Brachialis	10.79
Brachioradialis	2.32

Interpreting the results from Table III and Table IV, the forearm and hand have a total resistive weight of 4.5 lbf and the total maximum output force from the biceps brachii, brachialis, and brachioradialis is 20.2 lbf. However, the parameters of interest are the torques required by both the hand and elbow motor. Rather than choosing motors that can mimic the total maximum output force by the biceps brachii, brachialis, and brachioradialis, it is much more practical to choose motors that can overcome the resistive weights of the forearm and hand.

The elbow motor has to counteract both the elbow and hand, while the hand motor just has to counteract the weight of the hand. The torque on each of these motors is the weights they have to overcome multiplied by the radius of the reels the motors are attached to. These values can be found in Table V.

TABLE V  
TORQUES ON MOTOR

	Large Motor	Small Motor
<b>Force To Overcome (lbf)</b>	4.5	1.22
<b>Reel Radius (in)</b>	.59	.35
<b>Torque (lbf*in)</b>	2.71	.427

The torques are provided in units of lbf\*in, however the specification sheets for the motors provide their torque limits in units of kgf\*cm. For the sake of convenience, the torques on the larger motor and small motor are 3.12 kgf\*cm and .491 kgf\*cm, respectively.

It is important to note that rotation of the lower arm and hand will be achieved through the use of cables. These cables will be placed on the arm and will act at an angle that is separate from the angle of rotation of the arm. The horizontal component of the forces on the cables will induce a torque on the motors as can be shown in Figure 15.

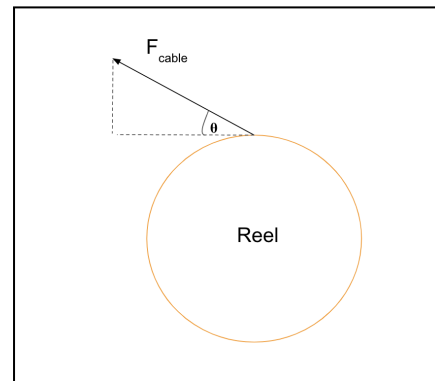


Fig. 15 Diagram depicting how cables will be acting at an angle to the reel that houses the motors. The horizontal component of the force induces a torque about the center.

The cables will be pulling against the weights of the forearm and hand, however it is the vertical component of the weights that make a right angle to the horizontal component of the cable, producing a torque. Thus, the maximum torque is when the horizontal component of the cable is exactly 90 degrees to the vertical component of the weights. This occurs when the hand is positioned as it is depicted in Figure 13. There is no torque when the arm is straight down to the side or rotated fully up to the shoulder because the cable force and weights will be fully in-line with one another. If the angle of zero degrees is taken to be when the arm is positioned as is depicted in Figure 14, and the arm can rotate either 90 degrees above or below, then the maximum weight force will be at 0 degrees, and this will also be the position at which the torque on the motors is the greatest. The graph in Figure 16 depicts this motion, and as hypothesized, the weights are the greatest when the arm is at the zero-degree position.

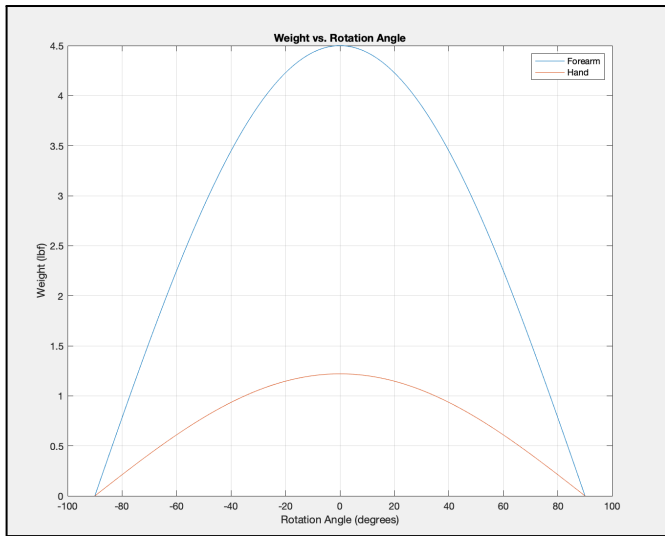


Fig. 16 Graph of the force vs the rotation angle about the elbow. The weight from the forearm is in blue and the weight of the hand is in red

### C. Controls

The movement is controlled via two motors with built-in encoders and two drivers. The Pololu 19:1 Metal Gearmotor 37Dx68L is used to control the flexion and extension of the elbow. With a maximum torque of  $8.5 \text{ kgf} \cdot \text{cm}$  and a 64 CPR encoder built-in, the motor communicates with a Pololu VNH5019 Motor Driver Carrier to execute this motion. The hand motor is the Pololu Romi/TI-RSLK MAX, and utilizes a built-in encoder and an identical motor driver. The stall torque on the hand motor is at  $4.5\text{V } 1.8 \text{ kgf} \cdot \text{cm}$  which is well above the torque expected to be on the hand motor from the calculations above. PID control was utilized for both motions as can be seen in Figure 17.

The circuit board is outlined in Fig. 9 and includes two Arduino nanos, connections to both motors and their drivers, a push button, and a power source. Two Arduinos were necessary because a single one only had two interrupt pins, which was not enough to accommodate the signals from two encoders and a push button. The interrupt pin is used to track the input from the push button and lets the Arduino know that the user wants to stop or start a phase of motion. Similarly, motor position, as indicated by encoder tracking, is obtained via interrupts. In addition, trying to run multiple interrupts at once was inconsistent and created errors. So, using multiple Arduinos in communication via I2C allowed the second Arduino to act as a parallel processor, and continuously loop through and check encoder information for both of the motors. The main Arduino was able to call to the motor position as needed and still accurately track the button interrupt.

The Arduinos are uploaded with a code that controls both motors through five phases controlled by the user's input of the push button. The first phase is triggered by supplying the power source to the circuit board through a switch in the backpack. The user puts on the backpack while the code waits for the push button as a trigger for the next phase. Once the button is pressed for the first time, phase two begins where the elbow begins to flex slowly using PID motor control to control the speed. The button is pressed once the maximum desired flexion angle is reached, and this angle is saved by the encoder and phase three begins. Next, the elbow is slowly extended using the same logic until the maximum extension is achieved and the button is pressed. A sine wave is scaled to

these flexion and extension values to act as the target in phase four, the main phase. Repetitions for the flexion/extension motion of the elbow and grasping and extending motion of the hand are performed every 10 seconds following the sine wave previously found. When the therapy is complete, pressing the button triggers phase five, where both Bowden cables are returned to their neutral position and the machine stops.

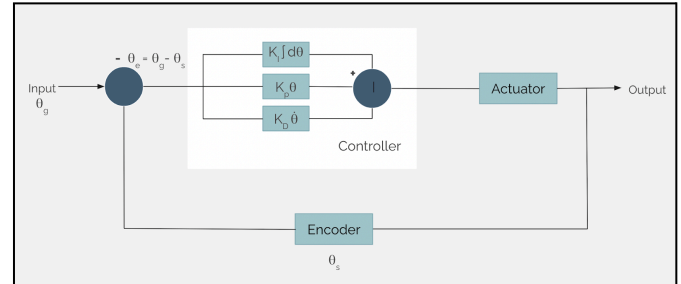


Fig. 17 Control diagram

### III. IMPLEMENTATION

The implementation phase of the design took place during the Spring 2024 semester.

#### D. Assembly

Final materials, including bowden cables and adhesives were purchased at the beginning of the semester. The reels and backpack insert were 3D printed, and the reels were tested to ensure a snug fit on the respective motors. First, the Arduino code on the motors was tested to ensure that they function with correct speed and continuity before attaching them onto the completed textile component of the exoskeleton. Once all components were acquired and the code was tested, assembly of the apparatus commenced.

A hole was cut and sewn in the wrist cuff to provide a location to attach the adjustable chord. The Arduino code was troubleshooted and revised until the spool turned in the correct sinusoidal manner and the on and off button was functional. Additionally, a through pass for the bowden cable was 3D-printed and attached to the breadboard, to ensure a secure motion in one direction.

For the hand grasping and ungrasping design, the chord was fused to the 3D printed spool. The hand motor was attached to the breadboard and the sinusoidal input was synchronized with the elbow motor.

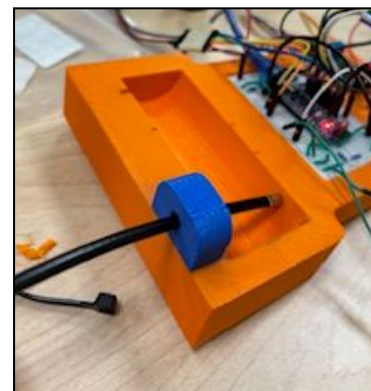


Fig. 18 3D-printed through-pass for Bowden cable.

### E. Testing

The original design for the exoskeleton was driven by a single Arduino Nano. Preliminary testing of the large motor was successful in creating oscillating motion with some inconsistency in the reading of the push button. This initially presented as a wiring issue, leading us to believe soldering wires to a circuit board would solve the inconsistency. When attempting to incorporate the hand motor, the code was unsuccessful due to a lack of interrupt pins on the Arduino Nano. The code requires five interrupt pins, two for each motor and one for the push button. During the initial testing, the large motor was mimicking the correct pattern, but the code was not running properly due to the lack of interrupt ports.

Utilizing PID motor control and interrupts allows both motors to run smoothly without jumping to positions, and respond quickly to button presses. To maintain the use of these two components a second Arduino Nano was added to the circuit and connected using I2C. This allowed for the second Arduino Nano to run as a constant loop supplying I2C information on hand and elbow motor positions.

The original breadboard was too small for the additional Arduino so it was replaced by a breadboard with twice the length. In the new breadboard circuit, wires were replaced by male to female cords which offered a more secure connection. These cords helped to ensure consistency by preventing loose connections or disconnections of wires from the breadboard. The larger breadboard was glued to the backpack insert and was too wide to fit within the backpack compartment. Velcro was used to secure the backpack insert to the outside of the backpack.

Initial testing of the circuit and motor assembly revealed an issue with the cord driving the elbow flexion and extension. The cord had a tendency to tangle around the exposed shaft of the large motor, disrupting the motion. This was resolved by designing a 3D printed part to feed the cord directly from its protective tubing to the motor reel at an optimal angle.

### G. Experiments and Results

Before fully assembling the prototype, the wiring was finished and the preliminary Arduino program was tested on the motors. The code was run successfully to control both motors. After running the code several times, assembly began on the final prototype. The larger breadboard did not fit inside the backpack's main compartment, so a velcro strap was used to secure the backpack insert to the outside of the backpack.

The fully assembled prototype was tested on a group member to evaluate the motors' ability to overcome the resistance of the arm and fingers. At this point it was discovered that the small motor did not have enough power to overcome the resistive forces in the hand. The calculations of the resistive force did not account for the addition of elastics on the back of the fingers, which create additional force acting against the grasping motion.

While it was unable to provide the full desired range of motion, the motor was able to cause the fingers to deflect slightly in the desired direction. When the hand cable is detached from the fingertips it runs as expected. Additionally,

other components like the large motor give us confidence that with a stronger hand motor, the design can run effectively.



Fig. 19 Front, side, and back view of final Exoskeleton Prototype

## IV. CONCLUSIONS

### A. Goal Assessment

The S.U.R.E prototype achieved the majority of its goals. Execution of the elbow flexion and extension motion was achieved. The push button effectively commenced and stopped the rehabilitation exercises. This meets the goal of being intuitive for at-home individual use. The hand motor was functional and moved in a sinusoidal motion synchronously with the arm motor. When worn by research team members, the elastic additions on the glove pulled the fingers into the extended position, but the hand motor was not strong enough to complete the finger grasping and ungrasping motions. Additionally, the chord used for the hand motor was too rigid and did not effectively cling to the motor reel.

The total weight of the apparatus came in at 3.15 lbs, nearly 40% below the target maximum weight of 5 lbs. This weight could be reduced further by using a slimmer 3D printed mount and less dense fill in the 3D printing process.

The final cost of the prototype came in at \$440. This is \$140 above the goal budget. The majority of this came from the 3D printing process. The prototype's price could be reduced by using a less dense fill and a slimmer Arduino and 3D printed mount. Further research could be conducted to find different options for the motors, glove, and backpack at lower prices. Production of this design would allow for bulk purchasing of components, reducing the cost per model. Additionally, in large scale manufacturing, more cost effective forms of manufacturing than 3D printing would be used.

The team members who modeled the final prototype attested to the comfort and wearability of the glove and backpack, meeting the ergonomics design goal. The final design is comfortable and adjustable between users and sessions for extended periods of time. The fit of the glove promotes extension in its natural elastic state.

### B. Future Work

The prototype, although mostly functional, could benefit from future work. In future iterations, the 3D printed mount will use much less filament to better fit new components, as well as reduce the cost. This will also reduce the weight of the design. A motor will be ordered that is strong enough to support the hand grasping, even with the elastic on the fingers. Although the code is in place to perform this action, the motor itself did not provide enough torque. This will likely be more



expensive than the current motor encoder assembly being used, but it is important to the functionality of the machine and its ability to improve fine motor abilities. The circuit board will be fully soldered instead of using removable pins. This will reduce the size of the breadboard needed so it will fit in the backpack and make it more reliable, since pins and wires being pulled out will no longer be an issue. Finally, professionals in the fields of exoskeleton design and stroke rehabilitation will be consulted to get qualitative feedback on the design after the initial rounds of testing. In the future, it is possible that IRB-approved studies could be done to test the efficacy for actual stroke patients.

## V. REFERENCES

- [1] An, K. N., Linscheid, R. L., & P. W. Brand, P. W. (1991). Correlation of physiological cross-sectional areas of muscle and tendon. *Journal of Hand Surgery*, 16(1), 66–67. [https://doi.org/10.1016/0266-7681\(91\)90130-g](https://doi.org/10.1016/0266-7681(91)90130-g)
- [2] Centers for Disease Control and Prevention. (2021). FASTSTATS - body measurements. <https://www.cdc.gov/nchs/fastats/body-measurements.htm>
- [3] Dinh, B. K., Xiloyannis, M., Cappello, L., Antuvan, C. W., Yen., & S. Masia, L. (2017). Adaptive backlash compensation in upper limb soft wearable exoskeletons. *Robotics and Autonomous Systems*, 92, 173-186. <https://doi.org/10.1016/j.robot.2017.03.012>
- [4] Herman, I. P. (2007). *Physics of the human body*. Springer-Verlag. <https://doi.org/10.1007/978-3-319-23932-3>
- [5] Hosseini, M., Meattini, R., San-Millan A., Palli, G., Melchiorri C., Paik J. (2020). A sEMG-Driven Soft ExoSuit Based on Twisted String Actuators for Elbow Assistive Applications. *IEEE Robotics and Automation Letters*, 5(3), 4094-4101. <https://doi.org/10.1109/LRA.2020.2988152>
- [6] Lin, L., Zhang, F., Yang, L., & Fu, Y. (2021). Design and modeling of a hybrid soft-rigid hand exoskeleton for poststroke rehabilitation. *International Journal of Mechanical Sciences*, 212. <https://doi.org/10.1016/j.ijmecsci.2021.106831>
- [7] O'Dell, M. W., Lin, C. -C. D. & Harrison, V. (2009). Stroke Rehabilitation: Strategies to Enhance Motor Recovery. *Annual Review of Medicine*, 60(1), 55–68. <https://doi.org/10.1146/annurev.med.60.042707.104248>
- [8] O'Neill, C., Proietti, T., Nuckols K., Clarke M. E., Hohimer C. J., Cloutier A., Lin, D. J., Walsh, C. J. (2020). Inflatable Soft Wearable Robot for Reducing Therapist Fatigue During Upper Extremity Rehabilitation in Severe Stroke. *IEEE Robotics and Automation Letters*, 5(3), 3899-3906. <https://doi.org/10.1109/LRA.2020.2982861>
- [9] Patel, P. (2023). Practical Exosuit Design for Patients With Amyotrophic Lateral Sclerosis; Investigating the Relationship Between Exoskeleton Designers and Their Users. Charlottesville, VA: University of Virginia, School of Engineering and Applied Science. <https://doi.org/10.18130/19ky-rm49>
- [10] Plagenhoef, S., Evans, F. G., & Abdelnour, T. (1983). Anatomical data for analyzing human motion. *Research Quarterly for Exercise and Sport*, 54(2), 169–178. <https://doi.org/10.1080/02701367.1983.10605290>
- [11] Sugar, T. G., He, J., Koeneman, E. J., Koeneman, J. B., Herman, R., Huang, H., Schultz, R. S., Herring, D. E., Wanberg, J., Balasubramanian, S., Swenson, P., & Ward, J. A. (2007). Design and Control of RUPERT: A Device for Robotic Upper Extremity Repetitive Therapy. *IEEE Transactions on Neural Systems and Rehabilitation Engineering*, 15(3), 336–346. <https://doi.org/10.1109/TNSRE.2007.903903>
- [12] Van Meijeren-Pont, W., Tamminga, S. J., Goossens, P. H., Groeneveld, I. F., Arwert, H., Meesters, J. J. L., Mishre, R. R., Vliet-Vlieland, T. P. M., van den Hout, W. B. (2021). Societal burden of stroke rehabilitation: Costs and health outcomes after admission to stroke rehabilitation. *Journal of Rehabilitation Medicine*, 53(6). <https://doi.org/10.2340/16501977-2829>
- [13] American Heart Association. (2022). U.S. stroke rate declining in adults 75 and older, yet rising in adults 49 and younger. <https://newsroom.heart.org/news/u-s-stroke-rate-declining-in-adults-75-and-older-yet-rising-in-adults-49-and-younger>
- [14] Franceschini, M., Mazzoleni, F., Goffredo M., Pournajaf, S., Galafate, D., Criscuolo, S., Agosti, M., Posteraro, F. (2020). Upper limb robot-assisted rehabilitation versus physical therapy on subacute stroke patients: A follow-up study. *Journal of Bodywork and Movement Therapies*, 24(1). <https://doi.org/10.1016/j.jbmt.2019.03.016>